Reviewer 2

The authors presented a reactive MD study of soot inception and early surface growth during acetylene pyrolysis at four temperatures between 1350 and 1800 K relevant to typical hydrocarbon flames. The objective of this study is to provide a more general view of soot inception by investigating the evolution of a reaction system containing C2H2 molecules, rather than assuming some intermediate species or PAHs as the initial condition.

1. Overall, the analysis and discussion of the results are comprehensive and offer useful insights into chemical evolution of the simulation system associated with soot inception and early surface growth. However, it is somewhat disappointed to notice that the authors did not provide the details of soot inception, such as the precursor species involved, even though their results should be able to provide such details by examining the numerical results slightly prior to the occurrence of the soot particle shown in Fig. 1.

1. This is probably a misunderstanding. In Fig. 5 of the original manuscript, we have provided the temporal evolution of C_2, C, C_2H_4, C_4H_2, CH_4, CH_3, C_2H_3, C_2H, C_2H_6, and C_2H_5, which correspond to the most abundant hydrocarbon species at the onset of surface growth. There, i.e., at 0.8 ns for 1650 and 1800 K, at 3.65 ns for 1500 K and at 5.2 ns for 1350 K, the amount of C_2H_4, C_2H_3, and C_2H molecules peaks, before it drops at 1 ns for 1650 and 1800 K, 4 ns for 1500 K and 5.5 ns respectively after the onset of surface growth, indicating that these species may significantly contribute to the growth of incipient soot nanoparticle but not necessarily to the inception process.

      To further address the Reviewer's Comment, we have discussed the importance of specific precursor species in the soot formation pathways in the end of p. 14 and in p. 15 of the revised manuscript: "The concentration of all molecules increases while C_2H_2 is rapidly consumed (Fig. 3a). At the onset of surface growth, C_2H_3 exhibits the highest concentration (Fig. 5d, solid line), suggesting that the intermediates formed by reactive collisions of acetylene are eventually converted to vinyl radicals, as proposed in the hydrogen abstraction vinyl acetylene addition (HAVA) mechanism (Shukla 2012).

      For example, at T = 1350 K, the C_2H_3 (Fig. 5d) and C_2H_4 exhibit a peak (Fig. 5b) at t = 5.25 ns, which corresponds to the timestep right after the onset of the surface growth (Fig. 3). There (t = 5.25 ns), only a small amount of C_2H (Fig. 5d), C_4H_2 (Fig. 5b), C_2, C (Fig. 5a), and H_2 (Fig. 5f) is produced, followed by an increase in CH_3 and CH_4 (Fig. 5c) at $t \geq$ 5.5 ns, indicating that the primary products during acetylene pyrolysis (such as C_2H_3, C_2H_4) also contribute to the formation of hydrocarbon molecules containing > 5 C. The role of C_2H_3 has also been highlighted in kinetic mechanisms as a key contributing molecule to the formation of cyclopentadiene through its addition to C_4H_6, which competes with benzene formation pathways and influences the composition and growth of soot particles (Faravelli, Goldaniga and Ranzi 1998). The amount of C_2H_4 (Fig. 5b: solid lines), CH_4 (Fig. 5c: solid lines), C_2H_6 (Fig. 5e: solid lines), and H_2 (Fig. 5f: solid lines) hardly changes at longer times, after C_2H_2 has practically been depleted, indicating that these species do not contribute to the growth of the soot cluster. The abrupt decrease in C_2H_4 (Fig. 5b: solid lines), C_2H_3 (Fig. 5d: solid lines) and C_2H concentration (Fig. 5b: broken lines) also hints that these species contribute towards the growth of incipient soot. It should be noted that the contribution of polyynes, such as C_4H_2 and C_2H, has also been recognized in accelerating polymerization reactions that lead to soot nucleation (Indarto 2008)."

      In addition, the detailed list of molecules and their chemical structure slightly prior to the occurrence of the soot nanoparticle has been provided for T = 1350 K in Table S4 at t = 5 ns (i.e., 0.2 ns prior to the onset of surface growth), as well as for T = 1650 and 1800 K in Tables S7 and S12, respectively, at t = 0.8 ns (i.e., 0.05 ns prior to the onset of surface growth). To clarify this, the 1st and 2nd paragraph in p. 21 of the revised manuscript have been modified as follows: "... (Supporting Information: Table S3). For 1350 K at t = 5 ns (Supporting Information: Table S4), 3-member rings and molecules containing > 5 C atoms are formed, coinciding with C_2H_2 consumption (Fig. 3a). At this temperature, hardly any 5- and 6-member rings are found in the reported chemical structures (Supporting Information: Tables S3-S6), which exclude the incipient soot, indicating that most of these rings are formed within the incipient soot nanoparticle. Nevertheless, at t = 5 ns (i.e., 0.2 ns prior to the onset of surface growth), a molecule with a 6-member ring appears in the C_6-C_{10} range (Supporting Information: Table S4), but most of the larger molecules with > C_{10} are primarily long aliphatic chains.

      Smaller benzene derivatives are observed in the reaction pathway at 1650 (Tables S10-S11) and 1800 K

(Tables S14-S15). At both 1650 (Tables S7-S11) and 1800 K (Tables S12-S15), mostly 3-member rings are formed up to 6 ns along with the incipient soot (excluded in the tables). Approximately 0.05 ns prior to the onset of surface growth (Table S12: t = 0.75 ns), a 5-member ring spontaneously forms. At T = 1650 K,…".

2. The authors paid close attention to the evolution of 3-, 5-, and 6-member rings in their results, but did not mention if there are other polycyclic aromatic species in the system, such as 4- or 7-member rings.

2. We thank the Reviewer for this Comment. To address this, we have quantified the temporal evolution of the number of 4- and 7-member rings at various temperatures. Figure R1 shows that a negligible number of 4-member rings is formed transiently. These structures are rather unstable and practically disappear over time. In contrast, a considerable number of 7-member rings is formed, comparable to that of 5-member rings (Fig. 6b). All 7-member rings appear after the onset of surface growth and belong to the incipient soot nanoparticle.

Figure R1 has been inserted as Figure S16 in the revised Supporting Information. In addition, the following sentence has been added in the end of Section 2.3 of the revised manuscript: "The 4- and 7-member ring structures are determined by MAFIA-MD (Mukut, Roy and Goudeli 2022)." and the following clauses have been included in the paragraph in p. 16: "…and 1800 K (stars), with 4- and 7-member rings shown in Fig. S16. The …" and "…before the onset of surface growth, no 5-, 6- and 7-member rings are observed (Fig. 6 and S16), indicating…".
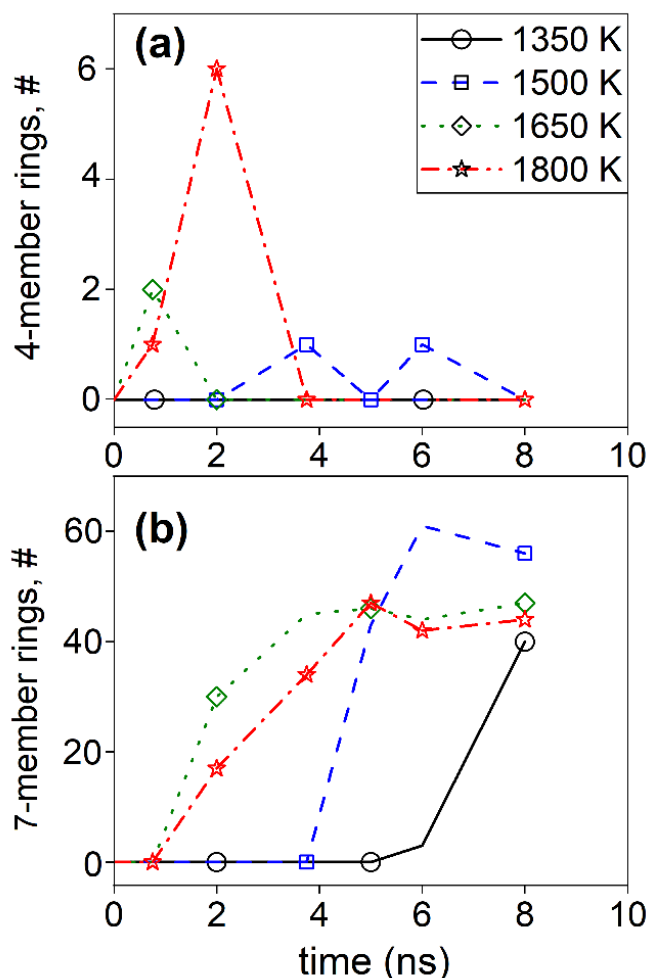

Figure R1. Temporal evolution of (a) 4- and (b) 7-member rings at 1350 (circles), 1500 (squares), 1650 (diamonds), and 1800 K (stars). A negligible number of 4-member rings is formed transiently, indicating that these structures are rather unstable and practically disappear over time. In contrast, a considerable number of 7-member rings is formed, comparable to that of 5-member rings (Fig. 6b). All 7-member rings appear after the onset of surface growth and belong to the incipient soot nanoparticle.

3. The authors also noticed that their results are somewhat different from those reported in the literature for different fuels and at different temperatures (Wang et al., 2022a, Wang et al., 2022b, Zhao et al., 2020). Can the authors speculate if the chemical details of soot formation and early growth will be different for different hydrocarbons?

3. We thank the Reviewer for raising this question. Indeed, soot formation pathways may differ depending on the fuel type, and nucleation conditions such as temperature and pressure (Richter and Howard 2000, Reizer, Viskolcz and Fiser 2022). Even though the detailed chemical structure of soot and its precursors are scarcely provided, to the best of our knowledge, the following qualitative insights can be obtained based on the literature:

The bulk ReaxFF literature focuses on high temperature conditions (>2400 K) that are more relevant to carbon black formation rather than to soot. For example, formation of carbonaceous nanoparticles during acetylene pyrolysis at high temperature (3000 K) has been explored by ReaxFF (Zhang et al. 2015) using the same forcefield as in the present study. The clusters and larger nanoparticles reported in this study (Fig. R2) resemble those obtained in our work (Fig. 1 in the revised manuscript), with large linear-like chains occupying the surface of the nanoparticle while islands of carbon rings occupy the cluster core (Fig. R2d-g).
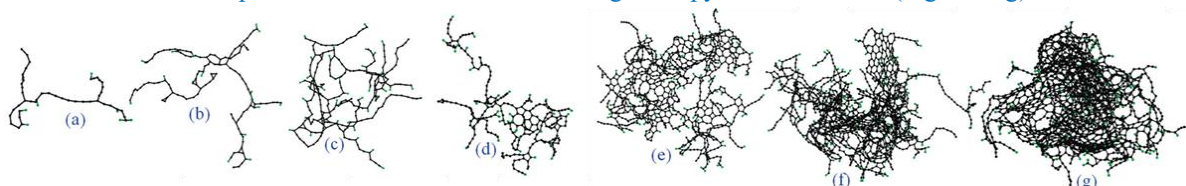

Figure R2. Typical structures showing the stages in carbon black formation (adjusted from (Zhang et al. 2015).

However, fuels such as n-decane and n-heptane, lead to compact onion-like soot nanoparticles with higher ring content and shorter aliphatic side chains compared to soot structures obtained by acetylene pyrolysis at the same temperature range (Fig. R2). For example, pyrolysis of n-decane at 3000 K (Liu et al. 2020) has revealed the formation of PAH-like structures (Fig. R3). During thermal degradation at 3000 K, n-decane decomposes into smaller molecules such as CH_4, C_2H_4, and C_2H_3, consistent with those observed in the present work (Fig. 5). Reactive collisions gradually result in PAH-like molecules and larger soot nanoparticles with graphitic-like structure. These results are consistent with those obtained by n-heptane pyrolysis at $T = 2200 - 2600$ K in Fig. R4 (Fakharnezhad et al. 2025), indicating that the fuel type can significantly affect the formation mechanism and structure of soot.
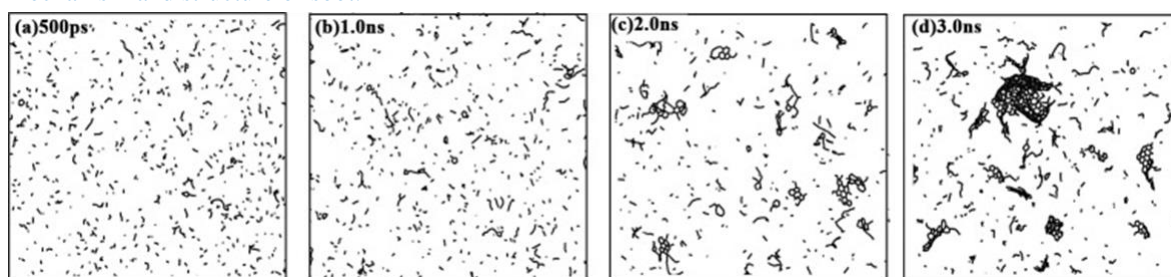

Figure R3. Snapshots during soot formation by n-decane pyrolysis at 3000 K (adjusted from (Liu et al. 2020)).
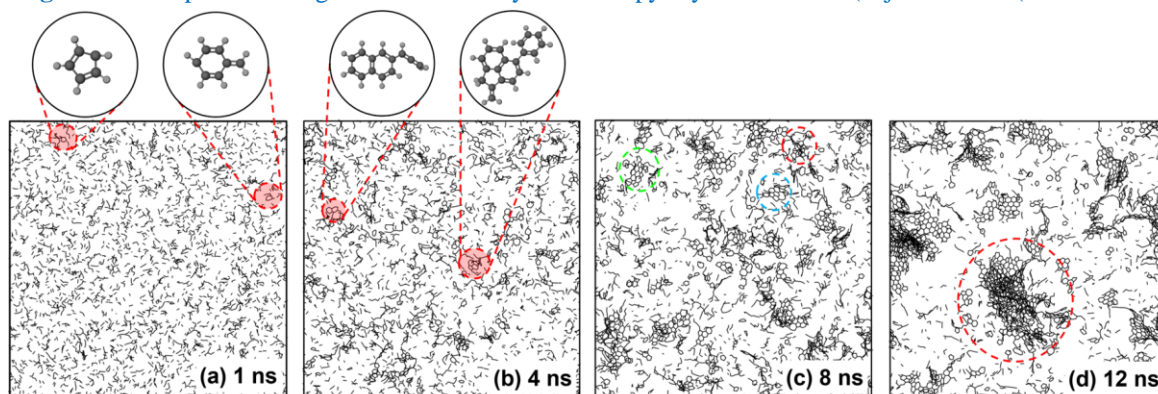

Figure R4. Snapshots of soot formation by n-heptane pyrolysis at 2500 K (Fakharnezhad et al. 2025).

To clarify this, we have modified the end of the last paragraph of p. 21 of the revised manuscript as follows: "…It should also be noted that at temperatures below 1800 K, which are relevant to soot formation in flames, the ReaxFF-predicted cluster structures are significantly different from those formed by acetylene combustion at 2700 K (Wang et al. 2022a), by methane and ethylene combustion at 3000 K (Wang et al. 2022b), by dimerization of PAHs (Zhao et al. 2020), and by pyrolysis of n-decane at 3000 K (Liu et al. 2020) n-heptane at 2200 – 2600 K (Fakharnezhad et al. 2025), where PAH-like soot precursors are formed leading to large carbonaceous clusters mainly composed of rings and containing only a small fraction of branches. This indicates that the fuel type along with the nucleation conditions can significantly affect the formation mechanism and structure of soot.".

Minor points:

• *In line 17 on page 3, 'shoot' should be soot.*

Corrected.

• *In the line below Fig. 5, why do you call the results in Fig. 6 'the cumulative number …' rather than 'the number …'?*

Thank you. We have replaced "the cumulative number" with "the number".

• *In the first paragraph on page 16, Figure S15a and Figure 15b seem messed up.*

Thank you. We corrected the caption of Figure S15 of the original manuscript (Figure S17 in the revised Supplementary Information).

References

Fakharnezhad, A., D. M. Saad, G. A. Kelesidis & E. Goudeli (2025) Nucleation Rate of Soot by n-Heptane Pyrolysis. *Aerosol Science & Technology,* accepted.

Faravelli, T., A. Goldaniga & E. Ranzi (1998) The kinetic modeling of soot precursors in ethylene flames. *Symposium (International) on Combustion,* 27, 1489-1495.

Indarto, A. (2008) Soot Growth Mechanisms from Polyynes. *Environmental Engineering Science,* 26, 1685-1691.

Liu, L., H. Xu, Q. Zhu, H. Ren & X. Li (2020) Soot formation of n-decane pyrolysis: A mechanistic view from ReaxFF molecular dynamics simulation. *Chemical Physics Letters,* 760, 137983.

Mukut, K. M., S. Roy & E. Goudeli (2022) Molecular arrangement and fringe identification and analysis from molecular dynamics (MAFIA-MD): A tool for analyzing the molecular structures formed during reactive molecular dynamics simulation of hydrocarbons. *Computer Physics Communications,* 276, 108325.

Reizer, E., B. Viskolcz & B. Fiser (2022) Formation and growth mechanisms of polycyclic aromatic hydrocarbons: A mini-review. *Chemosphere,* 291, 132793.

Richter, H. & J. B. Howard (2000) Formation of polycyclic aromatic hydrocarbons and their growth to soot—a review of chemical reaction pathways. *Progress in Energy and Combustion Science,* 26, 565-608.

Shukla, B. a. K., Mitsuo (2012) A novel route for PAH growth in HACA based mechanisms. *Combustion and Flame,* 159, 3589-3596.

Wang, Y., M. Gu, D. Liu & X. Huang (2022a) Soot growth mechanism in C2H2 combustion with H2 addition: A reactive molecular dynamics study. *International Journal of Hydrogen Energy.*

Wang, Y., M. Gu, Y. Zhu, L. Cao, J. Wu, Y. Lin & X. Huang (2022b) Analysis of soot formation of CH4 and C2H4 with H2 addition via ReaxFF molecular dynamics and pyrolysis–gas chromatography/mass spectrometry. *Journal of the Energy Institute,* 100, 177-188.

Zhang, C., C. Zhang, Y. Ma & X. Xue (2015) Imaging the C black formation by acetylene pyrolysis with molecular reactive force field simulations. *Physical Chemistry Chemical Physics,* 17, 11469-11480.

Zhao, J., Y. Lin, K. Huang, M. Gu, K. Lu, P. Chen, Y. Wang & B. Zhu (2020) Study on soot evolution under different hydrogen addition conditions at high temperature by ReaxFF molecular dynamics. *Fuel,* 262, 116677.